PCIM Europe 2024; International Exhibition and Conference for Power Electronics, Intelligent Motion, Renewable Energy and Energy Management; Proceedings of

Protection and Control of a Dual MMC Medium Voltage Supply

M. Dupont and D. Dujic

POWER ELECTRONICS LABORATORY
ÉCOLE POLYTECHNIQUE FÉDÉRALE DE LAUSANNE

 DOI: 10.30420/566262011

pcim EUROPE

Protection and Control of a Dual MMC Medium Voltage Supply

Max Dupont, Drazen Dujic

École Polytechnique Fédérale de Lausanne (EPFL), Power Electronics Laboratory, Switzerland

Corresponding author/speaker: Max Dupont, max.dupont@epfl.ch

Abstract

The Modular Multilevel Converter (MMC) is a mature technology for high and medium voltage AC to DC power conversion. In the majority of applications, the MMC is interfacing well-defined voltage levels on either side. Contrary to that, this paper presents the use of the MMC as a bipolar DC power supply, operating both as a voltage or current source. Control methods ensuring correct operation while respecting operational voltage and current limits on the DC side are presented. Furthermore, results are validated on a single MMC, and extended to two MMC units connected in series/parallel on the DC side, using RT-HIL simulations.

1 Introduction

Due to its realization based on the series connection of low-voltage submodules, the Modular Multilevel Converter (MMC), initially introduced in [1], [2], is characterized by exceptional voltage scalability, high efficiency, and good output voltage quality. These features led to the adoption of this technology in applications such as High Voltage Direct Current transmission (HVDC) [3], Medium Voltage (MV) drives [4], railway interties [5], and more. Additionally, the MMC intrinsically features di/dt limiting in case of DC short circuit thanks to its branch inductors, which is especially advantageous for MV or HV DC applications. Moreover, when full-bridge submodules are used, the short circuit currents can be further limited and even completely canceled. A demonstration of this can be found in [6], [7], where the authors provide experimental results gathered on a medium voltage MMC rated for 1.25 MW.

While this feature was used for the particular case of DC short circuits, the same principles apply to the limitation of the MMC output current for any kind of overload conditions. This allows the MMC to provide the same current limiting behavior as many other laboratory power supplies.

Identifying this, the dual MMC based converter of Fig. 1 was realized as a flexible 4 quadrant (4Q) medium voltage supply. Its two MMCs can be configured in series or parallel at the DC terminals, thanks to galvanic isolation on the AC side. In these configurations, illustrated in Fig. 2, the supply shall be usable as both a voltage source or a current source with current/voltage limiting, respectively. Due to various disturbances and parameter variations in a real system (detailed in section 4), the series current sources and parallel voltage sources operation require additional control to ensure equal power-sharing.

In the existing literature, very little can be found regarding such configurations. In bipolar HVDC systems, series connection of MMCs is common, but a neutral conductor is generally included [8], [9]. This midpoint connection absorbs the small current mismatches which are the cause of power unbalances seen in the true series connection of current sources. In truly series connected systems, the MMCs are treated as open loop controlled voltage sources, and the problem is solved by implementing the DC current controller centrally [9]. However, this solution introduces communication delays, which need to be minimized when fast current limiting is desired, as in the case of the laboratory supply. Similarly, the use of parallel connected MMCs is seldom discussed, and existing works address the current control of parallel connected MMCs, MMCs with parallel legs, or branches [10]–[12], but in all cases, the DC bus is assumed to be controlled externally. Consequently, the power-sharing challenge appearing in the parallel connection of voltage controlling MMCs is

ISBN 978-3-8007-6262-0

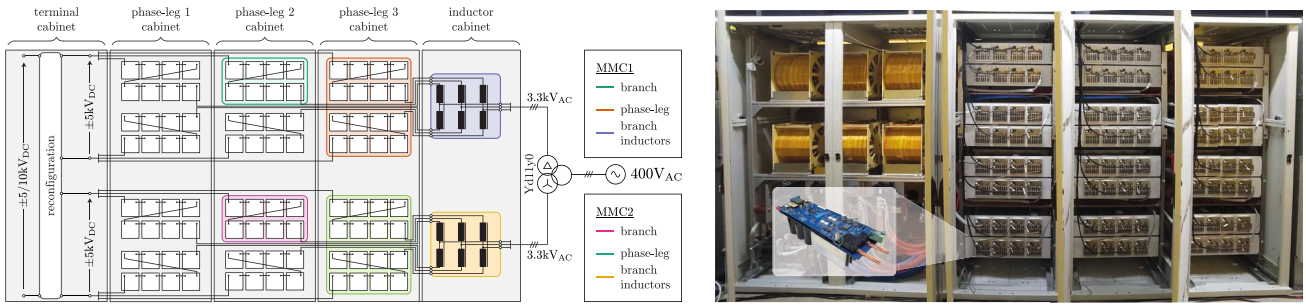

(a) (b)

Fig. 1: (a) Layout of the dual MMC based 4Q MV supply. (b) Actual realization with zoomed in view of a submodule.

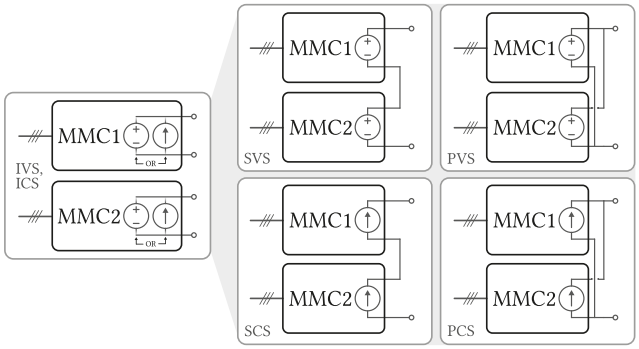

Fig. 2: MV supply internal configurations consisting of individual MMCs or series/parallel connected MMCs operated as voltage or current sources.

not addressed. Only studies on the 5 MW supply, based on four MMCs, which inspired this work, have proposed a master controller based solution, allowing arbitrary power-sharing in series/parallel configurations [13], [14].

Hence, this paper addresses the control and control based protection of a dual MMC four quadrant-supply rated for 500 kW, ±10 kV (Fig. 1). Its operation as a voltage or current source with user selected voltage and current limits is first detailed in the case of a single MMC, and extended to two units.

2 MV Supply Specifications

The realized MV supply (Fig. 1) is composed of two identical MMCs of which the key parameters are summarized in Table 1. At their DC terminals, the MMCs can be configured in series for ratings of $\pm 10\mathrm{kV}$, $50\mathrm{A}$, or in parallel for $\pm 5\mathrm{kV}$, $100\mathrm{A}$. This flexibility allows for covering a wide range of use cases without oversizing the converter's components. Since full-bridge submodules are used, the supply can operate in all four quadrants, and the full operating range is illustrated by the green areas in Fig. 3. Furthermore, by manipulating voltage and current limits, the operation of the power supply can easily be confined to a smaller operational area than the maximum allowed one, and examples of possible user-defined limits are illustrated by the orange boxes in Fig. 3. This functionality is valuable for protecting the supply and the device being supplied. For instance, when supplying a unidirectional converter, the voltage should be restricted to positive values, and negative currents prevented. The realization of such constraints using a control-based implementation is explained in the next section.

Tab. 1: Parameters of a single MMC.

MMC		Submodule	
P_{nom} [kW]	250	Type	Full bridge
$V_{\mathrm{DC,nom}}$ [kV]	± 5	Nb/branch	8
$V_{\mathrm{AC,nom}}$ [kV]	± 3.3	PWM	Unipolar
$f_{\mathrm{sw,eq}}$ [kHz]	16	f_{sw} [kHz]	1
L_{br} [mH]	1.75	V_{nom} [V]	650
R_{br} [mΩ]	66.4	C_{SM} [mF]	2.25

3 Control of a Single MMC

3.1 Control structure overview

The MMC control structure used in this work, and depicted in Fig. 4, is adapted from [15], and leverages techniques proposed earlier in [16], [17]. It uses a cascaded implementation with two layers, and the control is divided according to three different objectives: the control of the MMC's total energy content, the balancing of this energy across branches, and control of the DC voltage or current.

To realize the first objective ① the outer loop uses a PI based controller to maintain the total energy

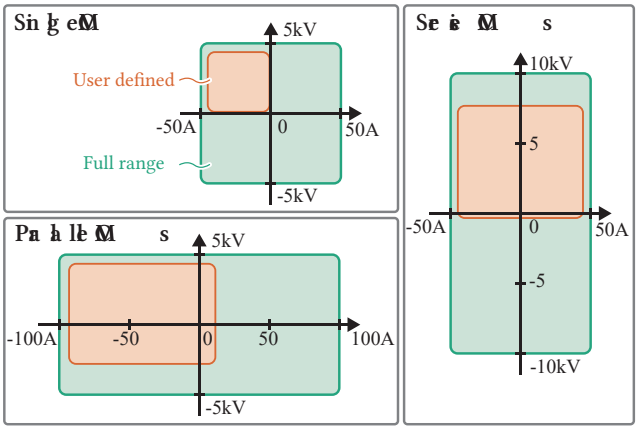

Fig. 3: Converter allowed operating range for all DC side configurations (green areas), and example of user-defined limits (orange areas).

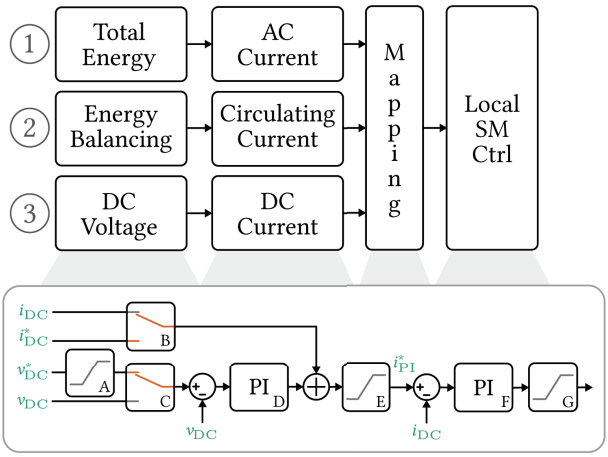

Fig. 4: MMC control structure, with details for the DC side control, which is the most relevant part for the features discussed in this work.

content of the converter to its desired value. Since the MMCs are used as rectifiers here, the output of this controller is a set of AC side current references used to exchange active power with the grid. An inner loop consisting of proportional resonant (PR) controllers at the fundamental, and 5th harmonics is used to track these references.

Energy balancing among the six branches of the MMC ② is ensured following the method of [17] and the output of this stage is a set of circulating current references. Another set of PR controllers tuned for the 1st and 2nd harmonics is used to track these references. The third set of controllers ③ is illustrated with more details as it is the most relevant part for the features discussed in this work. It consists of cascaded PI controllers to control the DC side current and voltage. Naturally, the outer loop voltage control is disabled when current source operation is desired.

All three objectives are achieved simultaneously, and the outputs of each current controller consist of voltage components that are mapped to form appropriate branch voltage references. These references are communicated to the submodules as modulation indices, where they are realized by phase-shifted carriers PWM, at the level of the branch. With modulation performed by the submodule controller, the balancing of submodules within a branch is also realized locally with a P controller as proposed in [16]. In addition, branch current references are also communicated to the submodules, where current control is enhanced by a local P controller.

3.2 DC side control

The DC side control structure, illustrated in the bottom part of Fig. 4, is realized to serve for current and voltage source operation, and selection is done by configuration of the signal selectors labeled ”B” and ”C”.

During operation as a voltage source, the signal selectors are configured in the upper position as in Fig. 4. External current references are ignored by replacing them with the current measurements, while voltage references are accepted, and the PI controller labeled ”D” is actively controlling the output voltage. In this instance, voltage limits are ensured by acting on the reference signal (saturation block ”A”). Moreover, the saturation block ”E” limits the reference entering the inner loop, effectively switching over to current source operation when a limit is reached. As a result, current limiting takes priority over voltage limiting in voltage source operation. The saturation limits of block ”G” are set to the maximum values allowed by the MMC and are only used for anti-windup of the PI labeled ”F”.

When operating the MMC as a current source, both selectors are in the bottom position. Hence, the voltage reference is replaced by the voltage measurement, and the error signal entering the PI controller ”D” is equal to zero, effectively switching it off. Only the inner current controller remains active, resulting in current source operation. In this configuration, current limiting is ensured by the saturation block ”E” which prevents the reference from exceed-

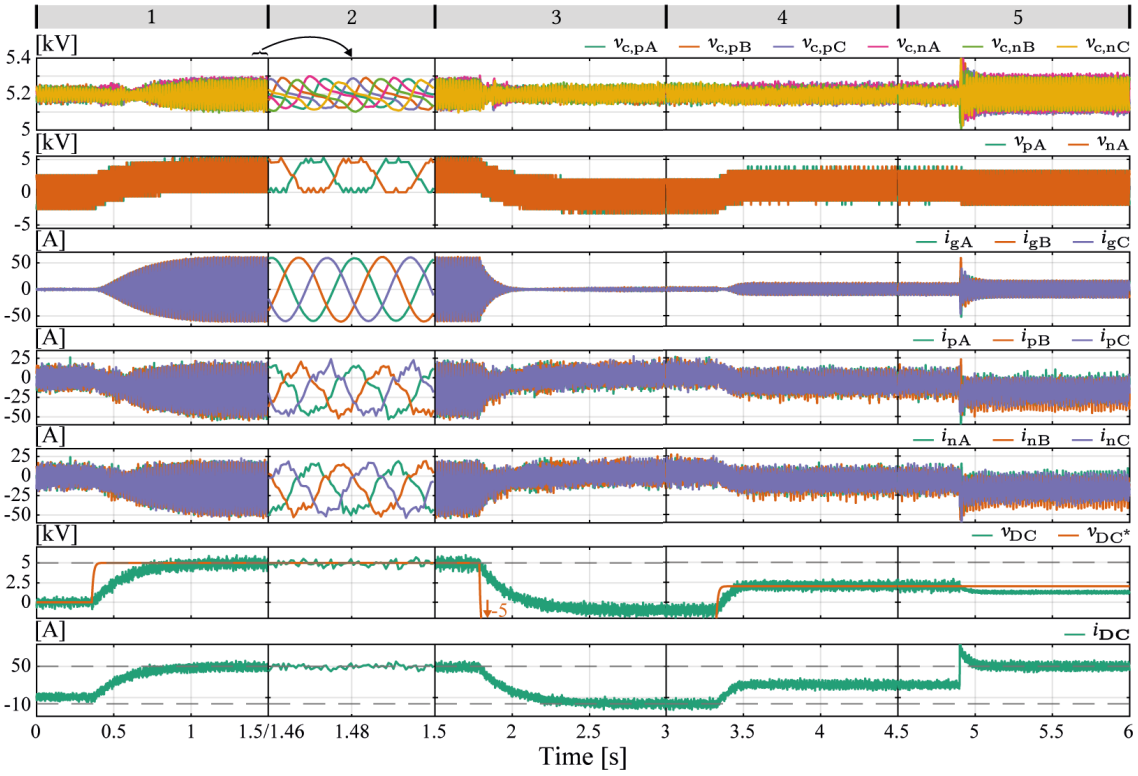

Fig. 5: RT-CHIL simulation results for a single MMC used as a voltage source. From top to bottom, the graphs show the sum of capacitor voltages per branches, the output voltage of the top and bottom branch of one phase leg, the AC terminal currents, the top branch currents, the bottom branch currents, the DC side output voltage, and DC side output current.

Fig. 6: RT-HIL test setup, detailed in [18].

ing previously defined limits, and voltage limiting is ensured by the saturation block ”G” which acts directly on the DC contribution of the branch voltage reference. Hence, in current source operation, voltage limits have priority over current limits.

3.3 Single MMC results

Figure 5 shows real time control hardware in the loop (RT-CHIL) simulation results for a single MMC operating as a voltage source. The waveforms are captured with the RT-CHIL setup shown in Fig. 6. This setup is divided into two cabinets,

Tab. 2: DC side control parameters.

Inner loop		Outer loop		Local	
K_p	1.11	K_p	0.07	$K_\mathrm{p,eq}$	1.33
K_i	511.8	K_i	0.001		
$f_\mathrm{s,central}$		8kHz		$f_\mathrm{s,SM}$	40kHz

each capable of simulating one MMC. Each MMC has 48 submodules and is simulated using seven PLEXIM RT Boxes, which interface with the central and submodule controllers. For dual MMC configurations, a 15th RT Box simulates the connection between the two MMCs and their load.

For the simulation of Fig. 5, the user-defined limits are set to $\pm 5\mathrm{kV}$, $[+50\mathrm{A}, -10\mathrm{A}]$, and the DC side control parameters used are listed in table 2 (note that $K_\mathrm{p,eq}$ is the equivalent contribution of the submodule's branch current controller to the DC side current control, acting in parallel to the central controller but with a faster sampling rate).

Initially, the MMC is turned ON and its DC voltage is regulated to zero. During the first segment, indi-

Fig. 7: Power unbalances in (a) series current source operation, and (b) parallel voltage source operation when no control action is taken to ensure power sharing.

cated on top, its voltage reference (second graph from the bottom) is stepped up to $+5\mathrm{kV}$ at nominal load. The zoomed-in steady-state waveforms shown in the second segment confirm the proper control of the MMC. The third segment shows a voltage reference step to $-5\mathrm{kV}$, however, the MMC does not reach this set point because the $-10\mathrm{A}$ current limit is reached before (bottom plot), and the MMC seamlessly switches to current control to satisfy this limit rather than track the voltage reference. In the fourth segment, the voltage reference is set to $+3\mathrm{kV}$, and the MMC switches back to voltage control and operates away from any limits. Finally, the last segment shows a sudden overload. After a brief overcurrent, the MMC manages to limit the current to $50\mathrm{A}$ within approximately $100\mathrm{ms}$.

4 Dual MMC Control

4.1 Series/parallel connection challenges

Among the possible dual MMC configurations (Fig. 2), series connection as voltage source (SVS) is relatively easy to achieve. The output voltage of each MMC can be set to half of the desired voltage, the current is defined by the load, and power is equally shared between the MMCs. Analogous considerations apply to the parallel connection of MMCs controlling their output current (PCS). In contrast, the series connection of current sources (SCS) and parallel connection of voltage sources (SVS) require more attention from the control point of view.

Problems arise because of the unavoidable measurement errors found in real systems, and offset errors are particularly problematic for dual MMC configurations. This issue is illustrated in the case of series connected current mode MMCs in Fig. 7a. In this example, MMC1 has a small negative offset in its current measurement, whereas MMC2's current measurement is correct. Assuming that the actual current flowing through both MMCs is initially equal to the desired value, which is $10\mathrm{A}$ in this example, the small current measurement error in MMC1 causes its controller to increase its output voltage. This increase leads to a current rise, and MMC2 detects a deviation from its setpoint and tries to counteract this change by decreasing its voltage. Eventually, MMC1 reaches its maximum output voltage, which is $5\mathrm{kV}$, and MMC2, which has not reached its negative voltage saturation limit, takes over the current control. Similarly, when paralleling MMCs as voltage sources (Fig. 7b), voltage measurement errors lead to uneven current sharing.

These problems are further illustrated by the RT-CHIL simulation results of Fig. 8. In particular, Fig. 8a shows the instant when all controllers of parallel connected voltage mode MMCs are enabled. At first, the branch sum voltages (two upper graphs) are upregulated to reach the desired total internal energy. This requires active power to be taken from the AC side, hence the large AC currents (two middle graphs) during this phase. During this initial transient, small disturbances are observed on the DC side, but immediately after, the MMCs' DC terminal currents diverge and saturate to their limits.

In contrast, unbalances in series connected current mode MMCs (Fig. 8b occur much slower. This can be explained by the fact that current measurements are more accurate than the output voltage measurements in this system; therefore, the parallel voltage source configuration is more affected. In Fig. 8b, a change of current reference was even necessary to observe uneven voltage sharing.

ISBN 978-3-8007-6262-0

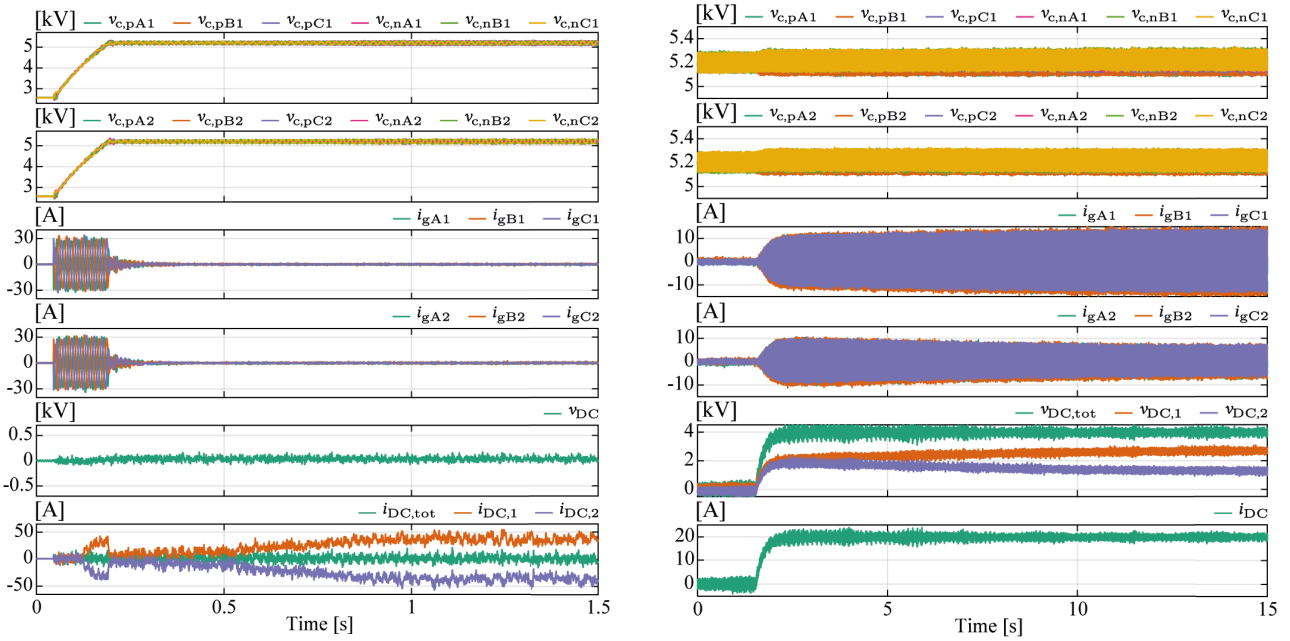

Fig. 8: RT-CHIL results showing power unbalances in (a) parallel voltage source operation, and (b) series current source operation when no control action is taken to ensure power sharing.

4.2 Master controller based solution

With an additional master controller monitoring the two MMCs, the DC side control structure discussed in section 3.2 can be leveraged to ensure equal power sharing. In particular, the signal selectors of Fig. 4 (blocks “B” and “C”) are configured to accept the current and voltage references sent by the master controller. Figure 9 illustrates how the master computes the references and how the MMCs use them.

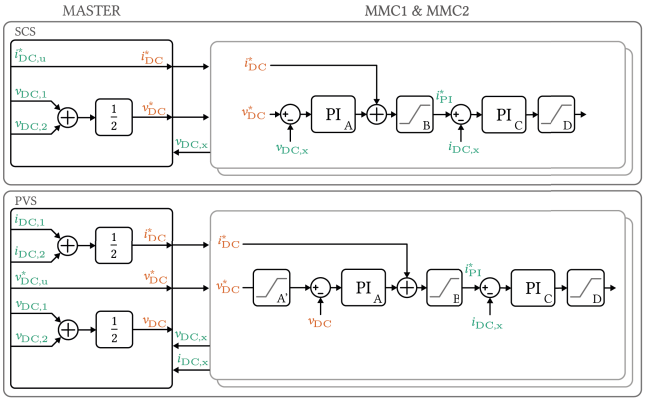

Fig. 9: Master controller based solution for power sharing in SCS and PVS.

The top part of Fig. 9 shows the calculations done in the master controller and the local DC side control structure configuration corresponding to the case of SCS. In this configuration, the user decides the current setpoint that is transmitted, as is, to both local MMC controllers. The outer voltage control loop guarantees voltage sharing among series connected MMCs by using their average output voltage as a reference. Essentially, the output of PI controller “A” compensates the measurement offset in $i_{\mathrm{DC,x}}$. The rest of the control remains identical to the case of a single current source MMC.

The bottom part of Fig. 9 illustrates the controller configuration used for PVS. The voltage setpoint, requested by the user, is transmitted to both MMCs. In the MMC controller, the local voltage feedback ($v_{\mathrm{DC,x}}$) is replaced by the average of voltage measurements provided by the master controller ($(v_{\mathrm{DC,1}} + v_{\mathrm{DC,2}})/2$). This ensures that both MMC controllers use the exact same voltage measurement, and the outputs of the PI controllers labeled ”A” in each MMC will not diverge. Additionally, the average output current is used to enforce equal current sharing.

For the SVS, the master controller communicates half of the voltage reference to each MMCs, and current is naturally determined by the load. Similarly, half of the current reference is sent to each MMC in the case of PCS.

5 RT-CHIL Simulation Results

The solutions discussed in the previous section are demonstrated through extensive RT-CHIL simulations of the complete system. While the power balancing issues mainly affect the SCS and PVS configurations, SVS and PCS are also simulated to ensure that a reasonable power balance is maintained even during current and voltage limiting.

5.1 Series current source MMCs

Starting with the case of series current mode MMCs, Fig. 10 presents simulated cases divided into four segments indicated above the graphs. Each segment presents a different transient and involves different limits. Throughout this RT-CHIL simulation, the control parameters of Table 2 are reused, and the user-defined limits are arbitrarily set to $[+8\mathrm{kV}, -3\mathrm{kV}]$, $[+40\mathrm{A}, -10\mathrm{A}]$.

Please note that the second graph from the bottom shows the output voltage of the supply and of each MMC. The plots of the MMC's outputs overlap, indicating excellent voltage sharing.

Initially, the MV supply is turned ON with a zero current reference. In the first segment, its reference (orange line in the bottom graph) is stepped to $+50\mathrm{A}$. However, the voltage and current limits are reached, and the converter only provides $+40\mathrm{A}$. In the second segment, its reference is changed to $-40\mathrm{A}$; this time, only the current limit constraints the output to $-10\mathrm{A}$. Then, in the third segment, the setpoint is changed again to $20\mathrm{A}$ and the supply operates away from any limit. Finally, in the fourth segment, an external voltage source is inserted in series with the load, disturbing the current control. To bring the current back toward the setpoint, the supply raises its output voltage, but the $+8\mathrm{kV}$ limit is reached. Like with a single MMC in current source mode, the voltage limit takes priority over current limits, and the converter settles with an output current violating the $-10\mathrm{A}$ limit. The new steady-state current is outside the user-defined limits but within the power supply's capability. For this example, the operation is maintained, but in a normal scenario, the supply would trip if the operating point is outside the user-defined limits for more than a predefined time limit.

In summary, this sequence shows that the master controller based solution maintains the same current and voltage limiting features as for a single MMC, while solving the issue of voltage sharing.

5.2 Series voltage source MMCs

A similar sequence is simulated for the case of series connected voltage source MMCs. The user-defined limits are arbitrarily set to $[+10\mathrm{kV}, 0\mathrm{kV}]$, $[+40\mathrm{A}, -40\mathrm{A}]$, and RT-CHIL results are shown in Fig. 11.

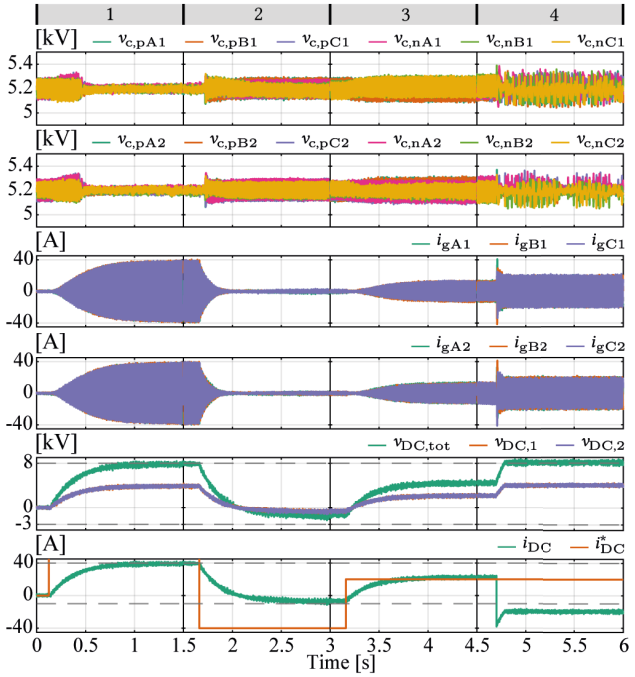

Fig. 10: RT-CHIL simulation results for SCS.

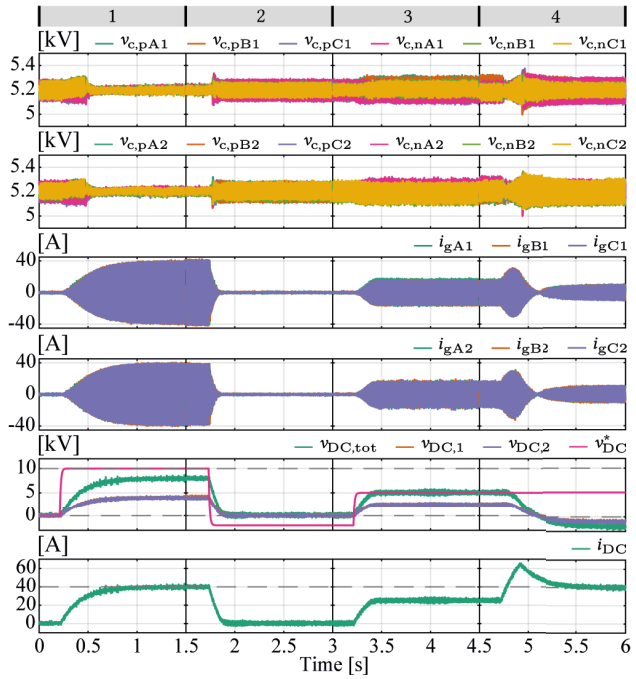

Fig. 11: RT-CHIL simulation results for SVS.

The sequence simulated is the following: The converter is initially turned ON with a voltage reference of $0\mathrm{V}$. In the first segment, the voltage reference (pink line in the second graph from the bottom) is changed to $+10\mathrm{kV}$. However, the output voltage of the converter (green line) does not reach this setpoint because the current limit is reached first (bottom graph). In the second segment, the voltage reference is changed to $-2\mathrm{kV}$. However, the previously defined voltage limit prevents the converter from following it, and the output settles at $0\mathrm{V}$. In the third segment, the setpoint is changed to $+5\mathrm{kV}$. This time, the converter can reach the setpoint and operates away from the current and voltage limits. In the last segment, a load change pushes the converter into current limiting mode, and the $0\mathrm{V}$ voltage limit is violated to allow the current limiting to work properly.

Throughout this simulation, the output voltages of the two MMCs are perfectly balanced (second graph from the bottom). This is natural for SVS, but this simulation also highlights that this balance is maintained during current limiting.

5.3 Parallel voltage source MMCs

Fig. 12 shows RT-CHIL simulation results for the case of parallel voltage source MMCs, when the user-defined limits are set to $[+5\mathrm{kV}, 0\mathrm{kV}]$, $[+50\mathrm{A}, -100\mathrm{A}]$.

The first segment illustrates a voltage reference step from $0\mathrm{V}$ to $+5\mathrm{kV}$. Constrained by the current limit of $+50\mathrm{A}$, the voltage settles at $2.5\mathrm{kV}$. In the second segment, due to a load change, the MV supply, which was delivering power, starts absorbing it. In these new conditions, the current is now far from the limit and the supply reaches its $5\mathrm{kV}$ setpoint. In the third segment, this setpoint is then changed to $0\mathrm{V}$. This time, the converter is prevented from reaching its voltage reference due to the negative current limit. Finally, the third segment shows a new reference step to $3\mathrm{kV}$, bringing the converter's operating point away from the limits, and into normal operation.

The effectiveness of the presented method is once again demonstrated as the MMC's output current remained balanced during the whole simulation.

5.4 Parallel current source MMCs

Finally, the last set of RT-CHIL simulation results is shown in Fig. 13 for the case of parallel current source MMCs. The user-defined limits are set to $[0\mathrm{kV}, -5\mathrm{kV}]$, $[+50\mathrm{A}, -100\mathrm{A}]$.

The first segment illustrates a current reference step from $0\mathrm{A}$ to $-100\mathrm{A}$; no limit is encountered, and the output current reaches its reference. In the second segment, a voltage source is inserted in series with the load, which reduces

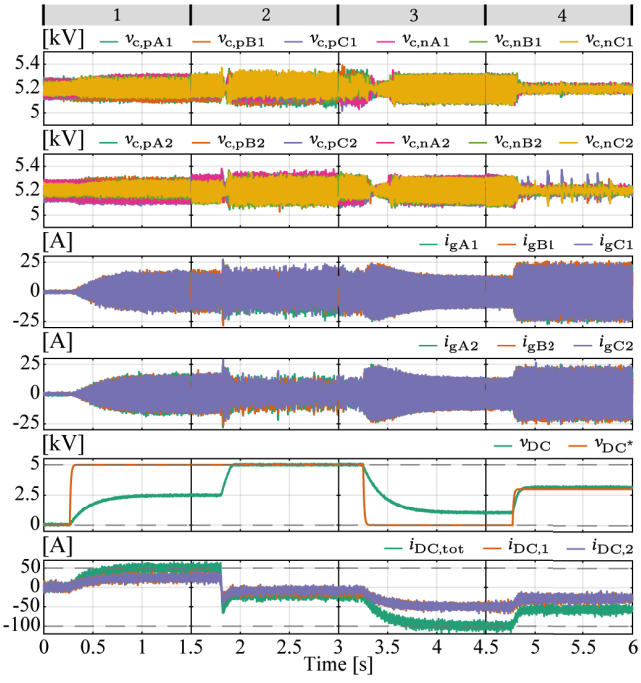

Fig. 12: RT-CHIL simulation results for PVS.

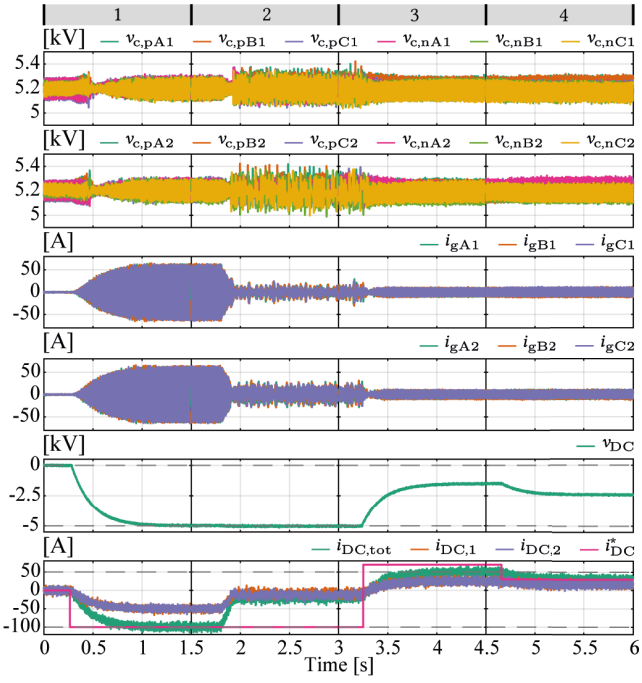

Fig. 13: RT-CHIL simulation results for PCS.

the output current. Since the MV supply was already operating at its maximum negative voltage, it could not bring the output current back toward the setpoint. In the third part of the sequence, the current reference is stepped to $+70\mathrm{A}$. As a result, the output voltage leaves its $-5\mathrm{kV}$ limit. Nevertheless, the new setpoint is not reached because it is outside of the user-defined current limits. Finally, the reference is changed to $+30\mathrm{A}$ and the converter settles about this new setpoint.

Similarly to the case of PVS, the output current of each MMC remained balanced, but this outcome was not guaranteed during voltage limiting. Indeed, when voltage limiting is in effect, the arrangement becomes one of parallel voltage sources, and the MMCs are essentially operated in open loop on the DC side. As a result, current imbalances are caused by differences in internal resistances between the two MMCs. Since these differences are negligible in this system, the current remained balanced.

6 Conclusion

This work presented a dual MMC-based MV converter system intended for use as a general-purpose laboratory supply. Its control-based implementation of current and voltage limiting was discussed and demonstrated for the case of a single MMC and extended to multi-MMC configurations. Challenges of voltage sharing in series connected current mode MMCs, and current sharing in parallel connected voltage mode MMCs were discussed. A master controller-based solution was presented and its efficacy demonstrated by extensive RT-CHIL simulations for all intended configurations of the MV supply. The current and voltage limiting features were thoroughly tested for each of these configurations, further demonstrating the seamless switchover ensured by this control-based implementation.

References

[1] A. Lesnicar and R. Marquardt, “An innovative modular multilevel converter topology suitable for a wide power range,” in *2003 IEEE Bologna Power Tech Conference Proceedings*, vol. 3, 2003, p. 6. DOI: 10.1109/PTC.2003.1304403.

[2] S. Allebrod, R. Hamerski, and R. Marquardt, “New transformerless, scalable Modular Multilevel Converters for HVDC-transmission,” in *2008 IEEE Power Electronics Specialists Conference*, 2008, pp. 174–179. DOI: 10.1109/PESC.2008.4591920.

[3] SIEMENS. “HVDC PLUS,” SIEMENS. (2012), [Online]. Available: https://p3.aprimocdn.net/siemensenergy/87cdd3cd-be98-4a79-b9c3-b03b00d3e37a/2022-03-11-HVDC-PLUS-pdf_Original%20file.pdf (visited on 12/22/2023).

[4] SIEMENS. “SINAMICS Perfect Harmony GH150,” SIEMENS. (2022), [Online]. Available: https://assets.new.siemens.com/siemens/assets/api/uuid:18aa6fa6-7bfa-450a-8328-2cfe787e8844/gh150acbrochurejune2019.pdf (visited on 03/14/2024).

[5] M. Winkelnkemper, A. Korn, and P. Steimer, “A modular direct converter for transformerless rail interties,” in *2010 IEEE International Symposium on Industrial Electronics*, 2010, pp. 562–567. DOI: 10.1109/ISIE.2010.5637826.

[6] M. Winkelnkemper, L. Schwager, P. Blaszczyk, M. Steurer, and D. Soto, “Short circuit output protection of MMC in voltage source control mode,” in *2016 IEEE Energy Conversion Congress and Exposition (ECCE)*, 2016, pp. 1–6. DOI: 10.1109/ECCE.2016.7855427.

[7] K. Sun, D. Soto, M. Steurer, and M. Faruque, “Experimental verification of limiting fault currents in MVDC systems by using modular multilevel converters,” in *2015 IEEE Electric Ship Technologies Symposium (ESTS)*, 2015, pp. 27–33. DOI: 10.1109/ESTS.2015.7157857.

[8] W. Guoqiang, W. Haiqing, Y. Rong, J. Lei, H. Ting, and L. Yu, “Dc resonance suppression for hybrid double-ended hvdc transmission systems,” in *12th IET International Conference on AC and DC Power Transmission (ACDC 2016)*, 2016, pp. 1–5. DOI: 10.1049/cp.2016.0392.

[9] C. Hirsching, M. Goertz, S. Wenig, S. Beckler, M. Suriyah, and T. Leibfried, “On control and balancing of mmc-hvdc links in rigid bipolar configuration,” in *15th IET International Conference on AC and DC Power Transmission (ACDC 2019)*, 2019, pp. 1–6. DOI: 10.1049/cp.2019.0026.

[10] F. Gao, D. Niu, H. Tian, C. Jia, N. Li, and Y. Zhao, “Control of Parallel-Connected Modular Multilevel Converters,” *IEEE Transactions on Power Electronics*, vol. 30, no. 1, pp. 372–386, 2015. DOI: 10.1109/TPEL.2014.2313333.

[11] J. Pou, S. Ceballos, G. Konstantinou, G. J. Capella, and V. G. Agelidis, “Control strategy to balance operation of parallel connected legs of modular multilevel converters,” in *2013 IEEE International Symposium on Industrial Electronics*, 2013, pp. 1–7. DOI: 10.1109/ISIE.2013.6563685.

[12] S. Milovanovic and D. Dujic, “On Power Scalability of Modular Multilevel Converters: Increasing Current Ratings Through Branch Paralleling,” *IEEE Power Electronics Magazine*, vol. 7, no. 2, pp. 53–63, 2020. DOI: 10.1109/MPEL.2020.2984350.

[13] P. Blaszczyk, M. Steurer, D. Soto, M. Bosworth, and M. Winkelnkemper, “Power balancing in multi-converter systems composed of modular multilevel converters (MMCs),” in *2016 18th European Conference on Power Electronics and Applications (EPE’16 ECCE Europe)*, 2016, pp. 1–10. DOI: 10.1109/EPE.2016.7695321.

[14] P. Blaszczyk, M. Winkelnkemper, and L. Schwager, “Converter energy balancing in MMC system energy sharing using master controller,” in *2015 International Conference on Electrical Drives and Power Electronics (EDPE)*, 2015, pp. 30–37. DOI: 10.1109/EDPE.2015.7325265.

[15] P. Blaszczyk, M. Steurer, D. Soto, F. Bogdan, J. Hauer, *et al.*, “Modular multilevel converter based test bed for MVDC applications — A case study with a 12 kV, 5 MW setup,” in *2016 IEEE International Power Electronics and Motion Control Conference (PEMC)*, 2016, pp. 139–145. DOI: 10.1109/EPEPEMC.2016.7751988.

[16] M. Hagiwara and H. Akagi, “Control and Experiment of Pulsewidth-Modulated Modular Multilevel Converters,” *IEEE Transactions on Power Electronics*, vol. 24, no. 7, pp. 1737–1746, 2009. DOI: 10.1109/TPEL.2009.2014236.

[17] J. Kolb, F. Kammerer, M. Gommeringer, and M. Braun, “Cascaded Control System of the Modular Multilevel Converter for Feeding Variable-Speed Drives,” *IEEE Transactions on Power Electronics*, vol. 30, no. 1, pp. 349–357, 2015. DOI: 10.1109/TPEL.2014.2299894.

[18] S. Milovanovic, I. Polanco, M. Utvic, and D. Dujic, “Flexible and efficient mmc digital twin realized with small-scale real-time simulators,” *IEEE Power Electronics Magazine*, vol. 8, no. 2, pp. 24–33, 2021. DOI: 10.1109/MPEL.2021.3075803.